MICROENCAPSULATION OF PROTEINS WITHIN $CACO_3$ MICROSPHERES USING SUPERCRITICAL CO_2 MEDIA

Leila N.HASSANI[1], Brice CALVIGNAC[1]*, Gaëtan J-R DELCROIX[1], My Kien TRAN[1], Thomas BEUVIER[2], François HINDRE[1], Alain GIBAUD[2], Frank BOURY[1]

[1]*Université d'Angers, INSERM U646-Ingénierie de la Vectorisation Particulaire, 49933 ANGERS Cedex 09, France*
[2]*Université du Maine, CNRS UMR 6087-Laboratoire de Physique de l'Etat Condensé, 72085 LE MANS Cedex 09, France*

brice.calvignac@univ-angers.fr

ABSTRACT
This study is a preliminary work of a global project aiming at conceiving and characterizing implantable synthetic extracellular matrices seeded with calcium carbonate multifunctional particles and releasing therapeutic biomolecules, for bone and cartilage tissue engineering. The formulation method of $CaCO_3$ microparticles is based on the formation of an emulsion of water in Sc-CO_2 (W/C). Hollow and spherical microparticles with a 5 µm diameter were successfully obtained and fully characterized. Encapsulation experiments were carried out using lysozyme as model protein. Encapsulation yield and lysozyme loading can reach respectively up to 60 % and 7 %. Moreover, protein release kinetics have been determined during 24 hours. Results were compared and discussed with the literature ones related to microencapsulation of lysozyme and other biomolecules within $CaCO_3$ particles. Hence, it permitted to bring out a proof of the concept of this emulsification process [1] for the encapsulation of model and therapeutic biomolecules.

Key words: calcium carbonate, supercritical CO_2, encapsulation, therapeutic protein, lysozyme

INTRODUCTION

Supercritical fluid (SCF) processes provide clean and efficient alternatives to several technologies such as extraction, chromatography, crystallization and material processing. Carbon dioxide (CO_2) is widely used as a SCF due to its non-toxicity and its easy reachable critical properties (P_c=7.38 MPa, T_c=304.35 K). Moreover, modifications in CO_2 temperature and pressure allow changing its physical properties, an interesting characteristic for the synthesis of calcium carbonate ($CaCO_3$) particles with a high degree of conversion [2,3]. Hollow calcium carbonate particles have attracted considerable attention owing to their excellent properties such as low density, high specific surface areas and porosity for drugs microencapsulation. Encapsulation processes of biomolecules involve many limitations because of the numerous interest molecules, which are heat and shear stress sensitive. Moreover, the use of potentially toxic compounds, such as organic solvents, is strictly regulated by authorities such as US Food and Drug Administration or European Pharmacopoeia that allow only traces in the final product. Indeed, these compounds may denature active molecules, therefore rendering classical encapsulation processes such as emulsion/solvent-extraction, coacervation or spray-drying poorly adequate. New processes aim at preserving the biological activity of the encapsulated molecules and permit to tune the encapsulation efficiency, together with an ap-

propriate release both *in vitro* and *in vivo*. The use of supercritical fluids technology seems to be a promising approach to reach these goals, with the possibility to avoid the use of deleterious or toxic compounds [4].
In this sense, Boury *et al.* patented a supercritical emulsification process which allows to produce calcium carbonate ($CaCO_3$) microspheres [1]. Calcium carbonate may be found in 3 anhydrous crystalline forms: vaterite, aragonite and calcite [5,6], all with different physical properties [7,8,9]. In the last decade, natural or synthesized calcium carbonate have been widely used in tissue engineering, for cartilage repair [10], but mainly for bone repair with carbonate scaffolds that advantageously substitute bone grafts by providing the 3D support required for an efficient repair [11,12]. Moreover, calcium carbonate is biodegradable and exhibits an excellent cytocompatibility, either alone [13] or when combined with other materials [14,15,16].
The aim of the present study is to give the proof of concept for the efficient encapsulation of a therapeutic protein within $CaCO_3$ microspheres. We focused on the synthesis of the mineral vector and the encapsulation of a model protein, lysozyme, within $CaCO_3$ microspheres produced in SC-CO_2 media. Hence, this study is the preliminary step of a global project aiming at the conception and the characterization of implantable synthetic extracellular matrices seeded with calcium carbonate multifunctional particles and releasing therapeutic biomolecules, for bone and cartilage tissue engineering.

MATERIALS AND METHOD

Carbonation reaction media. The synthesis method used in this study was patented and developed in our laboratory. The method is based on the formation of an emulsion of water in Sc-CO_2 (W/C) for which microdroplets acts as microreactors where several reactions succeed. Here, SC-CO_2 acts as a continuous (or external) phase and as reactant for the synthesis of $CaCO_3$ particles. The fast diffusion of CO_2 molecules into a basic aqueous solution leads to the formation ionic species such as HCO_3^- and CO_3^{2-} (Eq. 1 to 3). Then, the CO_3^{2-} ions react with Ca^{2+} ions to form calcium carbonate (Eq. 4) which may crystallizes under different polymorphs.

$$CO_2 + H_2O \leftrightarrow H_2CO_3 \leftrightarrow HCO_3^- + H^+ \quad \text{(Eq. 1)}$$

$$CO_2 + HO^- \leftrightarrow HCO_3^- \quad \text{(Eq. 2)}$$

$$HCO_3^- + HO^- \leftrightarrow CO_3^{2-} + H_2O \quad \text{(Eq. 3)}$$

$$CO_3^{2-} + Ca^{2+} \leftrightarrow CaCO_3 \quad \text{(Eq. 4)}$$

Preparation of aqueous solution. The aqueous solution used during this process contains 0.62 M NaCl (VWR international, Fontenay-sous-bois, France) and 0.62 M glycine (Sigma, Saint-Quentin-Fallavier, France) at a final pH of 10. Then, 1 % w/v calcium hydroxyde ($Ca(OH)_2$, Sigma) is added before adjusting the pH to 10 and filtering at 0.45 µm (Final concentration $Ca(OH)_2$: 0.8 %). Lastly, hyaluronic acid obtained from *Streptococcus equi.* (Sigma, average MW : 1630 kDa) is added (0,1 % w/v). The latter behaves as an anionic biopolymeric template for the formation of $CaCO_3$ microparticules that may direct the polymorphism of $CaCO_3$ particles similarly to what has been described using a similar molecule, chondroitin sulfate [17]. Glycine aims at favouring vaterite formation [18]. Encapsulation experiments were carried out using lysozyme as model protein, which was dissolved in the aqueous solution. Lyzosyme was obtained from chicken egg white (Sigma, average MW= 14 kDa).

Experimental set-up and procedure. A schematic diagram of the device used for $CaCO_3$ synthesis is shown in figure 5. The stainless autoclave (1) with a capacity of 500 mL (Separex, Champigneulles, France) is heated at 40.0 ± 0.1 °C and pressurized with CO_2 at 200 ± 1 bar. Liquid CO_2 is pumped by a high pressure membrane pump (Milton Roy Europe, Pont Saint Pierre, France) (2) and preheated by a heat exchanger (Separex, Champigneulles, France) (3) before feeding the autoclave equipped with a stirring mechanical device (Top-industrie, Vaux le Penil, France). The axis of the magnetic stirrer is equipped with an anchor stirrer and the stirring speed is 1200 rpm. Once, the equilibrium is reached (temperature and pressure constant), 25 mL of aqueous solution previously prepared are injected by means of an HPLC pump (Model 307, Gilson, Villiers le bel, France) (4). Injection flow is fixed to 10 $mL.min^{-1}$. Once addition is achieved, the final pressure is 240 ± 5 bar and stirring is maintained at 1200 rpm during 5 min. Thereafter, stirring is stopped and the autoclave depressurized at a rate of 40-50 bar/min.
Suspension of $CaCO_3$ microparticles is collected and centrifuged at 2400 g during 10 min. Lastly, microparticles are washed with 50 mL of ultrapure water (Milipore, Molsheim, France), centrifuged and lyophilised (Model Lyovax GT2, Steris, Mentor, USA) to obtain a dry powder of $CaCO_3$.

Figure 1. Schematic diagram of the experimental setup

Characterization techniques. X-ray diffraction (XRD) patterns were collected in reflection mode on powder spread out on a glass substrate. The measure was performed with a X-pert diffractometer using Cu-Kα radiation (λ = 1.54056A°) from 2□ = 10 to 70° in continuous mode with a step size of 0.07°. Scanning electron microscopy images (SEM; JEOL 6310F, Croissy sur Seine, France) were obtained with a tungsten cathode field emission gun operating at 3 kV on powder dispersed on a carbon scotch substrate. Atomic force microscopy measurements were performed with an Agilent 5500 AFM. All the topography images were realized in intermittent contact mode using the same PPP-NCHR-W tip (Nanosensors, Neuchatel, Switzerland). Image processing and grain size analysis were performed from SEM observations with the *Gwyddion* freeware. Transmission electron microscopy (TEM) studies were carried out (JEOL 2010, Croissy sur Seine, France) with a LaB_6 thermo-ionic emission source operating at 200 kV. The sample was dispersed in absolute ethanol and one droplet was deposited on a carbon-coated holey film supported by a copper grid before drying. The isothermal adsorption/desorption curves were recorded with an ASAP 2010 (Micrometrics, Norcross (GA), USA) system by using nitrogen gas. Prior to the determination of the isotherms, the physisorbed species are removed from the surface of the absorbent by exposing the sample to a high vacuum (5 µm Hg) at 100°C for 8h. Raman experiments were performed using a T64000 Raman spectrometer (Jobin–Yvon–Horiba, Lonjumeau, France) in a single monochromator mode. The excitation source was an argon–krypton ion laser (Coherent, Santa Clara (Ca), USA) operating at 514.5 nm.

Total protein quantification. The total lysozyme concentration in microparticles was determined by ELISA (Enzyme Linked Immunosorbent Assay). 5 mg of protein-loaded microspheres were dissolved by contact with 1.5 mL HCl 0.1 M for 10 min before dilution in phosphate buffer, pH 7.4, (DPBS, Lonza) to obtain a protein concentration in the range of 0-2 µg/mL. Insulin standard were prepared in PBS pH 7.4 from 0.1 to 2 µg/mL. 50 µL of samples or standards were incubated overnight at 4°C in Maxisorp™ plates (Nunc). After washing 2 times with DPBS, blocking was performed using 200 µL of DPBS, 1 % bovine serum albumin (BSA, Sigma) for 2 hours at room temperature. After blocking, wells were washed 2 times with DPBS before addition of i) 100 µL HRP-conjugated rabbit polyclonal anti-

lysozyme antibody (1:6500, Abcam, Paris, France) or ii) 100 µL primary anti-insulin rat monoclonal antibody (0.5 µg/mL, R&D systems, Lille, France). ii) After incubation at room temperature for 2 hours, wells were washed 3 times again before addition of 100 µL secondary anti-mouse IgG-HRP (0.5 µg/mL, R&D systems) and incubation for 1 hour at room temperature. After washing three times, revelation was performed using a substrate reagent pack (R&D systems) following the manufacturer's guidelines. After 5 min, reaction was stopped with 50 µL H_2SO_4 2N before measuring the optical density at 460 nm (Multiskan Labsystems).

Active protein quantification. The biologically active entrapped protein was determined using Micrococcus lysodeikticus. 30 mg of *M. Lysodeikticus* (Sigma) were placed in 200 ml TRIS NaCl buffer (pH 7.4) and incubated at 37°C for one hour. 5 mg of protein-loaded microspheres were dissolved by contact with 1.5 mL HCl 0.1 M for 10 min and diluted in TRIS NaCl buffer to reach a concentration of 0.1 to 1 µg/ml of lysozyme. 100 µl of samples or standards (0.1 to 1 µg/ml of lysozyme) were mixed with 2.9 mL of *M. Lysodeikticus* suspension in glass tubes (Kimble, Thermo Fisher Scientific) and incubated 4 hours at 37°C. Turbidity was finally assessed by measuring the absorbance at 450 nm (Kontron Uvikon 922, Northstar Scientific, Leeds, UK).

Protein release kinetic. 10 mg of microspheres were dispersed in 10 mL DPBS, at either pH 4.5, 6.0 or 7.4 and incubated in a water bath at 37°C under agitation (75 rpm). Samples were taken at 30, 60, 90, 120, 150, 180 min and 24 hours. At each sampling time, buffer was totally removed, microspheres washed once with ultrapure water before replacing buffer. Samples were diluted to obtain a final concentration of 0.1-1 µg/ml for lysozyme and 0.1-2 µg/ml for insulin. Quantification of the active lysozyme released was performed using the *Micrococcus lysodeikticus* assay while the ELISA assay was used for insulin release, as described in the previous sections. Release kinetics were performed in triplicate for each conditions.

Statistical analysis. All Data are presented as the mean value of 3 independent experiments ± standard deviation (SD), unless otherwise stated.

RESULTS AND DISCUSSION

Characterization of the $CaCO_3$ microspheres. In a first time, we focused on the study of structural and morphological characteristics of the $CaCO_3$ microparticles (without proteins) synthetized in supercritical CO_2.

Structural analysis. XR diffractogram of $CaCO_3$ particles (figure 2) shows that the main polymorph obtained is the vaterite (98 %mol). The peak at 29.3 ° is attributed to the most intense peak of calcite. Molar content of calcite is estimated about 2%. The presence of hyaluronic acid and glycine is supposed to support the formation of this thermodynamically non-stable $CaCO_3$ polymorph [19]. This one may have been driven by the presence of glycine in the aqueous solution [18], but may also vary depending on the experimental parameters. This issue is currently being investigated by *in-situ* studies using Raman spectroscopy and X-ray techniques (SAXS and WAXS).

Morphological analysis. SEM observations (figures 3a and 3b) indicate that $CaCO_3$ particles obtained are microspheres with a relatively narrow size distribution (average diameter = 4.9±1.0 μm). Figures (3b) and (3c) show particularly the external roughness and porosity of a particle. Its surface is composed of agglomerated nanograins. AFM observations (figure 4a) give information about the surface topography of a particle. Figure (4b) shows that nanograins average diameter is about 60 nm. Note that the grey bar refers to the height of the sample from 0 nm (in black) to 80 nm (in white). Each nanograins are probably composed of one or several agglomerated crystals of vaterite. This arrangement stabilize the particle and limits the transformation into the calcite polymorph.

SEM and TEM observations (respectively figures 3d and 3e) reveal that the microspheres structure is not homogenous and the centre of particles is less compact than its surface. Moreover, they show the presence of a hollow core and a shell with a radial morphology. Holes are present beyond of the hollow core. The holes concentration seems to gradually increase from the surface to the centre. BET analysis shows that the specific area of $CaCO_3$ particles is about 16 m^2/g (Figure 4). This high value for this type of particles (in comparison with literature) can be explained by the high specific of the agglomerated nanograins as well as by the accessible internal porosity. The adsorption and desorption isotherms show a pronounced hysteresis which is characteristic of a low coherent assembly of nanograins. Moreover, a Tensile Strength Effect (TSE) is observed during the nitrogen desorption when it exists a pore network and when interconnected larger pores (2 to 50 nm in the hollow core region) have to refill the smaller pores (inferior to 2 nm in the shell). Hence, these synthesis-conditions allow conferring a hollow structure to $CaCO_3$ microspheres and thus a promising capacity to the encapsulation applications.

Composition analysis. Raman analysis (figure. 6) confirms the obtention of vaterite polymorph and reveals the presence of some organic impurities such as glycine and hyaluronic acid. Indeed, in comparison with the Raman analysis of the pure organic components in the 2600-3400 cm^{-1} region, peaks are related to vibrations of ν(NH) at 3160-3230 cm^{-1} and ν(CH) at 2902, 2915 and 2962 cm^{-1}. Quantification of these components using the TGA-MS technique is currently under investigation.

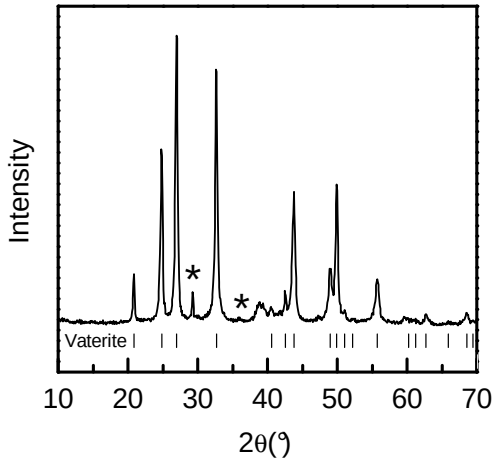

Figure 2. Structural analysis of XRD of the CaCO3 microspheres. Bragg reflexions of the vaterite polymorph (ICSD 15879) are indicated with vertical markers below the profile. *Calcite polymorph.

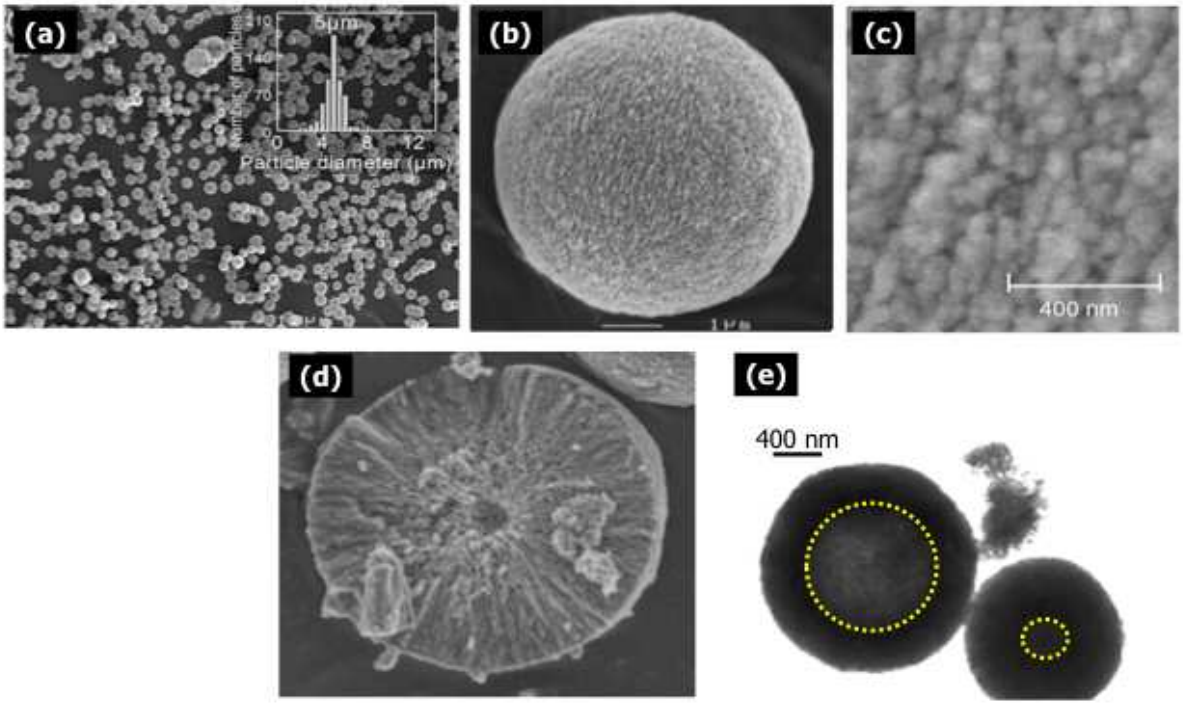

Figure 3. SEM (figures a to d) and TEM (e) observations of the $CaCO_3$ microparticles

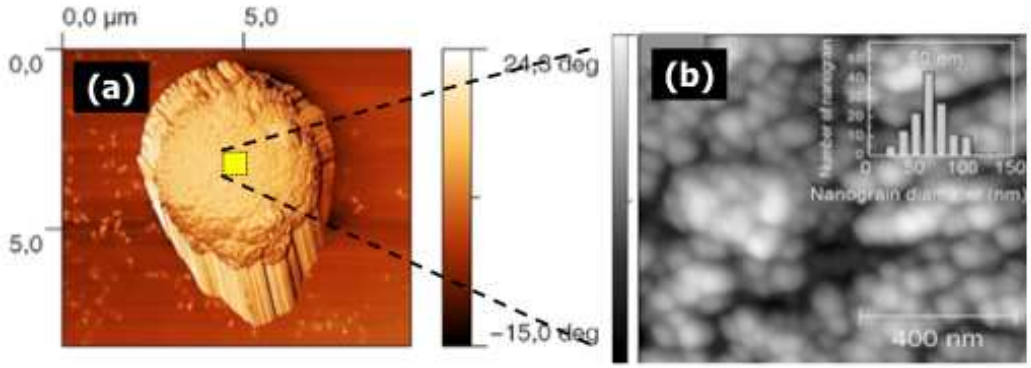

Figure 4. AFM observations of one particle and size measurement of its nanograins of vaterite

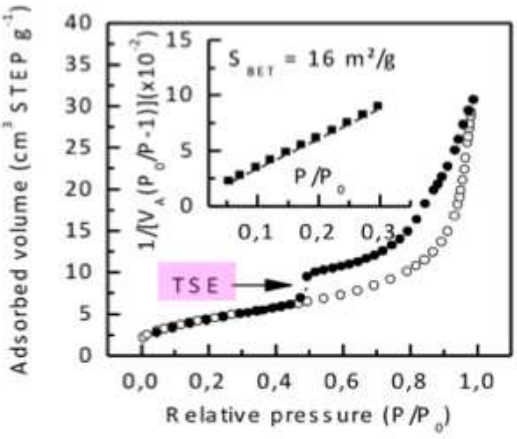

Figure 5. Nitrogen adsorption–desorption isotherms of the CaCO3 microspheres. The inset refers to the BET specific surface area analysis. Open and filled circles refer to adsorption and desorption isotherms. TSE: tensile strength effect

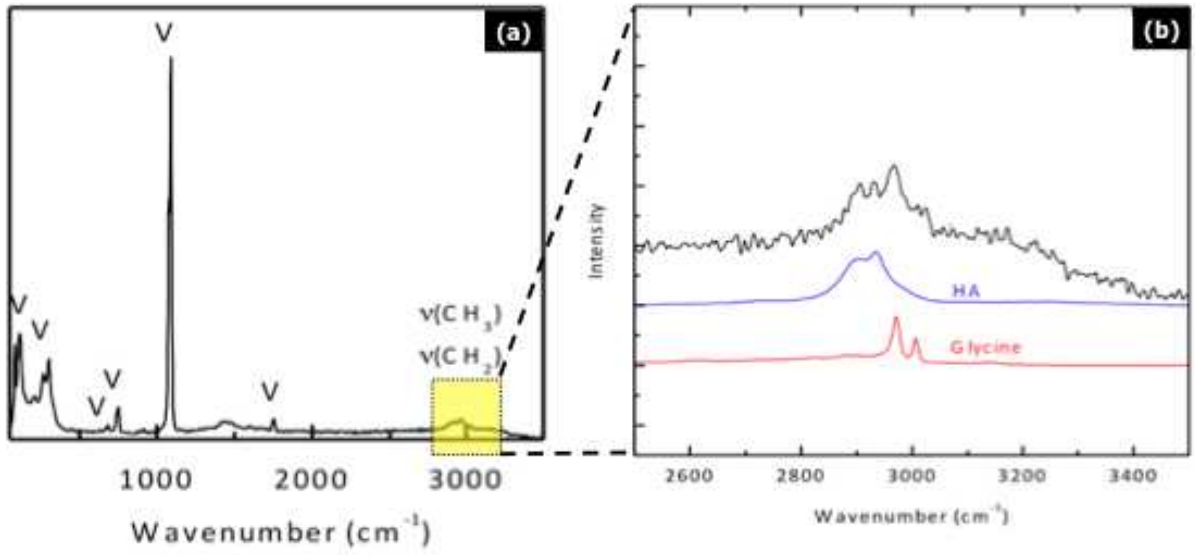

Figure 6. Raman spectrum of $CaCO_3$ microspheres (a) and magnification of the 2600-3400 cm^{-1} region (b)

Encapsulation of Lysozyme. In this study, chicken egg white lysozyme was used to provide a proof of concept of this encapsulation process with $CaCO_3$ particles. Presented results were obtained with a starting protein concentration of 0,5 and 1,0 g/L (Table 1). Firstly, it is important to note that the adding of lysozyme has no influence on the polymorphism (XR diffractogram not shown). Indeed, polymorphic composition (molar) is unchanged with respectively 98 % of vaterite and 2 % of calcite. On the other hand, lysozyme-loaded microspheres have a more stratified surface (figure 7c and 7d). It is supposed that the presence of lysozyme induces surface structural changes of $CaCO_3$ particles. Moreover, variations of zeta potential were observed which permits supposing that surface composition is modified too. Concerning these negative values, it could be attributed to the presence of anionic macromolecules such as hyaluronic acid and glycine. Raman analysis (data not shown) reveals too the presence of the organic components in the 2600-3400 cm^{-1} region as it was observed previoulsy.

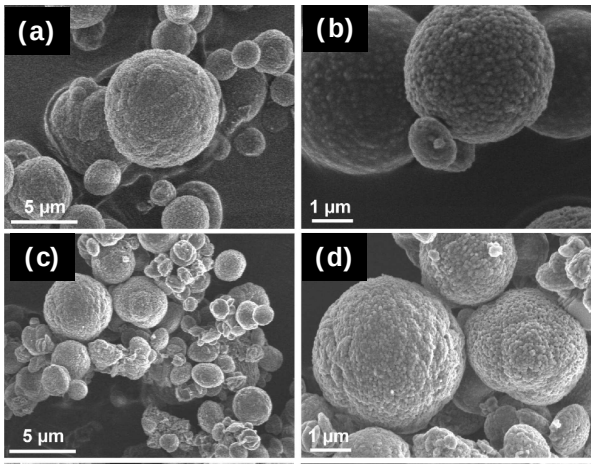

Figure 7. SEM observations of unloaded microspheres (a and b) protein-loaded (starting lysozyme concentration of 0.5 g/L) (c and d)

We successfully obtained $CaCO_3$ microspheres with a high protein loading (maximum around 7 %), a value higher [20] or similar to other study described in literature [21,22]. Note that these authors used processes involving the use of deleterious compounds such as organic solvents. Interestingly, a study described the encapsulation of small molecules as well as of proteins within $CaCO_3$ nanoparticles, but no loading nor encapsulation efficiency data were available in the case of the studied proteins [23]. An impregnation process of $CaCO_3$ microspheres after their formulation has been studied by Sukhorukov *et al.* [24]. However, the authors demonstrated that large molecules such as Dextran (4 kDa) could not diffuse deeply inside $CaCO_3$ microspheres. Noteworthy, these authors developed too a promising Layer-by-Layer (LbL) methodology, allowing the encapsulation of various molecules such as proteins within biocompatible microcapsules made from $CaCO_3$ microspheres [25]. Protein encapsulation yield in the case of lactalbumin (18 kDa) reaches up to 50 % [26]. Similarly, a LbL process was also used in another study to efficiently encapsulate a small molecule of interest for cancer therapy, doxorubicin [27], but with the drawback of being a time-consuming methodology. Fugiwara *et al.* [28] described an interfacial encapsulation method to encapsulate various proteins of increasing molecular weight such as BSA, ovalbumin and papain within $CaCO_3$ microspheres. Noteworthy, these authors demonstrated that the molecular weight of the protein to be encapsulated was proportional with the encapsulation yield. It seems to be the case for the studies previously cited. However, Fugiwara *et al.* [29] demonstrated that encapsulation of lysozyme was difficult using this method. Lysozyme loading was about 0.2 % with an encapsulation yield about 17 %. Note that particles obtained are no spherical and larger with a 10 µm diameter.

In this present study, and in addition to a high protein loading, high encapsulation efficiency was successfully obtained with a maximum value about 60 %. This yield may be improved by the optimization of the process during the depressurization step. Indeed, there are losses of solution (suspension composed of particles), from 10 to 20 % (vol.), which are drifted to the event during this step. This process improvement would consist in putting in place a trap with a capillary to collect the losses. Thus, suspension and CO_2 are separated and the last one is drifted to the event.

Finally, *Micrococcus lysodeikticus* assays show that this supercritical CO_2 encapsulation process permitted to retain up to 94 % of the biological activity of lysozyme for higher concentration of injected solution. This is consistent with a review from Wimmer *et al.* describing the effect of supercritical CO_2 on enzymes, which may even enhances the stability of under

denaturing conditions [30]. However, for 0.5 g/L concentration, protein activity is divided almost by three. Nevertheless, it is important to note that the lyophilisation step allows to store during long periods the particles without significant effects on the activity of encapsulated proteins.

Table 1. Lysozyme loading of microspheres and encapsulation yields of the process

Lyszyme concentration (g/L)	0 *	0.5	1.0
Active lysozyme loading (%)	/	1.2 ± 0.1	6.6 ± 0.1
Total lysozyme loading (%)	/	3.3 ± 0.5	7.0 ± 0.5
Encapsulation yield (%)	/	47.7 ± 6.6	59.8 ± 7.7
Average size (µm)	4.9 ± 0.3	4.9 ± 0.3	5.3 ± 0.3
Zeta potential (mV)	-21.5	-11.8	-15.2

** Experiences without Lysozyme*

Kinetic release of Lysozyme. This study was carried out on samples of experiments for lysozyme concentration at 0,5 g/L and at three different pH values: 7,4; 6,0; 4,5. A burst release was observed during the first 30 minutes of release, followed by a more progressive release that started to stabilize after 3 hours (figure 8). The amount of released proteins increased while lowering the pH, due to the faster degradation of $CaCO_3$ microspheres under acidic pH, and a maximum release of 89 % was obtained after 24 hours at pH 4.5. This degradation was observed at 24 hours of kinetic release using scanning electron microscopy (figure 8) despite a few crystalline artefacts probably due to lyophilisation required for sample preparation prior to scanning electron microscopy. Note that after 24 hours at pH 4.5, particles were totally dissolved and could not be observed anymore.

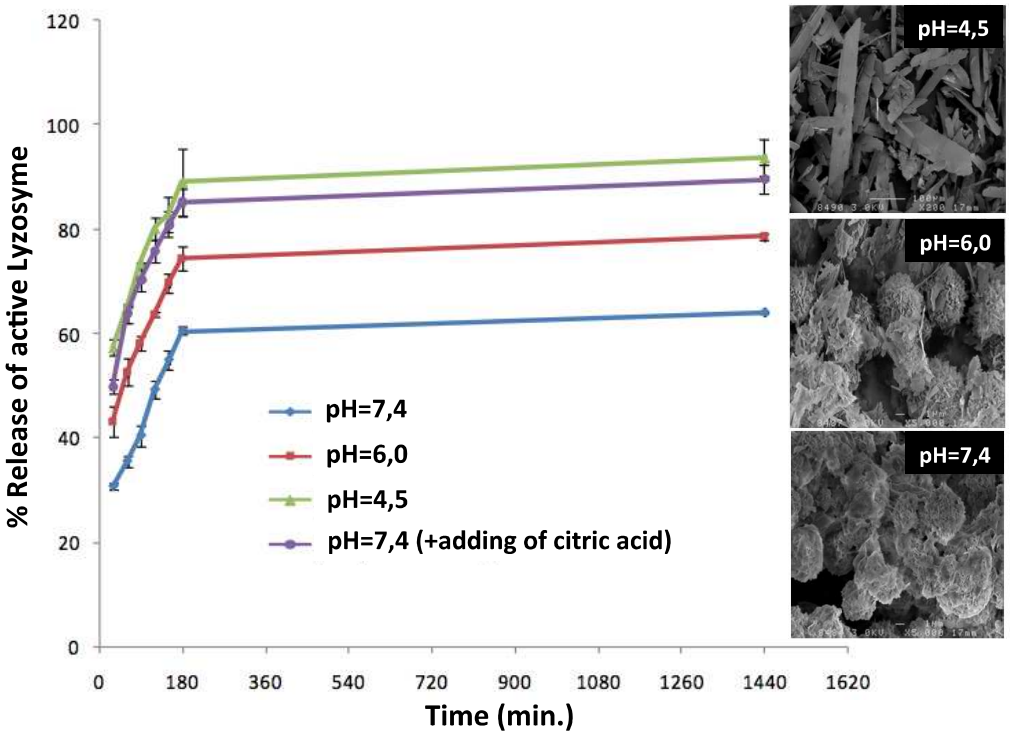

Figure 8. Lyzosyme kinetic release profiles and the corresponding SEM observations of microparticles after release

CONCLUSION

In the present work, it has been described a method for synthesizing calcium carbonate particles using SC-CO_2 in aqueous media. Hollow and spherical microparticles with a 5 µm diameter were successfully obtained and fully characterized. On the other hand, this work brings out a proof of the concept of new emulsification process for the encapsulation of model and therapeutic proteins such as lysozyme. It has been shown that the process allows obtain $CaCO_3$ microspheres with a protein loading up to 7 % and an encapsulation yield about 60 % which is improvable. Release of lysozyme is pH-dependent and reaches a maxima about 89 % at pH=4.5. On the other hand, a burst was observed during the first 30 minutes whatever the pH conditions.

Further study will consist to study the release of lysozyme in a cellulose-based polymer such as Si-HPMC (silanized hydroxypropylmethyl cellulose), which is an injectable biomaterial for tissue engineering. Then, study of encapsulation and release of transforming growth factor (TGF) will be carried out too. Thus, this work may generate promising results with regards to the elaboration of hybrid biomaterials composed of inorganic and organic compounds for biomedical applications.

ACKNOWLEDGEMENTS

The authors thank the financial support of ANR (France—Project ANR-09-PIRI-0004-01), Regional research program (Pays de Loire, France—Bioregos program) and the French education minister. The authors would like to thank the SCIAM laboratory (Angers, France) for SEM analysis.

REFERENCES

[1] Boury F., Benoit J.P., Thomas O., Tewes F., Method for preparing particles from an emulsion in supercritical or liquid CO2, **2005**, WO2007072106

[1] Gu W., Bousfiel D.W., Tripp C.P., J. Mater. Chem, 16, **2006**, p. 3312.

[2] Wakayama H., Hall S. R., Mann S., J. Mater. Chem., 15, **2005**, p. 1134.

[4] Debenedetti P.G., et al., Application of supercritical fluids for the production of sustained delivery devices. Journal of Controlled Release, 24(1-3), **1993**, p. 27.

[5] Domingo C., et al., Calcite precipitation by a high-pressure CO2 carbonation route, Journal of Supercritical Fluids, 36(3), **2006**, p. 202.

[6] Ouhenia S., et al., Synthesis of calcium carbonate polymorphs in the presence of polyacrylic acid. Journal of Crystal Growth, 310(11), **2008**. p. 2832.

[7] Kitamura M., et al., Controlling factors and mechanism of reactive crystallization of calcium carbonate polymorphs from calcium hydroxide suspensions. Journal of Crystal Growth, 236(1-3), **2002**. p. 323

[8] Mosharraf M., Sebhatu T., and Nyström C., The effects of disordered structure on the solubility and dissolution rates of some hydrophilic, sparingly soluble drugs. International Journal of Pharmaceutics, 177(1), **1999**. p. 29

[9] Gal J.-Y., et al., Calcium carbonate solubility: a reappraisal of scale formation and inhibition. Talanta, 43(9), **1996**. p. 1497.

[10] Kreklau B., et al., Tissue engineering of biphasic joint cartilage transplants. Biomaterials, 20(18), **1999**. p. 1743.

[11] Yukna R.A. and C.N. Yukna, A 5-year follow-up of 16 patients treated with coralline calcium carbonate (BIOCORAL) bone replacement grafts in infrabony defects. J Clin Periodontol, 25(12), **1998**, p. 1036.

[12] Soost F., et al., Natural coral calcium carbonate as alternative substitute in bone defects of the skull, Mund Kiefer Gesichtschir, 2(2), **1998**, p. 96.
[13] Combes C., et al., Preparation, physical-chemical characterisation and cytocompatibility of calcium carbonate cements. Biomaterials, 27(9), **2006**, p. 1945
[14] Schiller C., et al., Geometrically structured implants for cranial reconstruction made of biodegradable polyesters and calcium phosphate/calcium carbonate. Biomaterials, 25(7-8), **2004**, p. 1239.
[15] Combes C., Bareille R., and Rey C., Calcium carbonate-calcium phosphate mixed cement compositions for bone reconstruction. Journal of Biomedical Materials Research Part A, 79A(2), **2006**, p. 318.
[16] Wutticharoenmongkol P. et al., Preparation and characterization of novel bone scaffolds based on electrospun polycaprolactone fibers filled with nanoparticles. Macromol Biosci, 6(1), **2006**, p. 70.
[17] Manoli F. and E. Dalas, Spontaneous precipitation of calcium carbonate in the presence of chondroitin sulfate. Journal of Crystal Growth, 217(4), **2000**. p. 416.
[18] Shivkumara C., et al., Synthesis of vaterite CaCO3 by direct precipitation using glycine and l-alanine as directing agents. Materials Research Bulletin, 41(8), **2006**, p. 1455.
[19] Gopinath C.S., Hegde S.G., Ramaswamy A.V., Mahapatra S., Materials Research Bulletin, 37, **2002**, p. 1323
[20] Ungaro F. et al., Cyclodextrins in the production of large porous particles: development of dry powders for the sustained release of insulin to the lungs. Eur J Pharm Sci, 28(5), **2006**. p. 423.
[21] Amidi M. et al., Preparation and physicochemical characterization of supercritically dried insulin-loaded microparticles for pulmonary delivery. Eur J Pharm Biopharm, 68(2), **2008**, p. 191.
[22] Lee E.S. et al., Protein release behavior from porous microparticle with lysozyme/hyaluronate ionic complex. Colloids Surf B Biointerfaces, 55(1), **2007**. p. 125.
[23] Ueno Y. et al., Drug-incorporating calcium carbonate nanoparticles for a new delivery system. J Control Release, 103(1), **2005**, p. 93.
[24] Sukhorukov G.B. et al., Porous calcium carbonate microparticles as templates for encapsulation of bioactive compounds. J. Mater. Chem., 14, **2004**, p. 2073.
[25] Volodkin D.V. et al., Matrix polyelectrolyte microcapsules: new system for macromolecule encapsulation. Langmuir, 20(8), **2004**, p. 3398.
[26] Volodkin D.V., N.I. Larionova, and G.B. Sukhorukov, Protein encapsulation via porous CaCO3 microparticles templating. Biomacromolecules, 5(5), **2004**, p. 1962.
[27] Peng, C., Zhao Q., and Gao C., Sustained delivery of doxorubicin by porous CaCO3 and chitosan/alginate multilayers-coated CaCO3 microparticles. Colloids and Surfaces A: Physicochemical and Engineering Aspects, 353(2-3), **2010**, p. 132.
[28] Fujiwara M. et al., Calcium carbonate microcapsules encapsulating biomacromolecules. Chemical Engineering Journal, 137(1), **2008**, p. 14.
[29] Fujiwara M. et al., Encapsulation of Proteins into CaCO3 by Phase Transition from Vaterite to Calcite. Crystal Growth & Design, 10(9), **2010**, p. 4030.
[30] Wimmer Z. and M. Zarevucka, A review on the effects of supercritical carbon dioxide on enzyme activity. Int J Mol Sci., 11(1), **2010**, p. 233-53.